PIEZORESISTIVE MICRO-PILLAR SENSOR FOR IN-PLANE FORCE SENSING IN BIOLOGICAL APPLICATIONS

Isha Lodhi[1], Durga Gajula[2], Devin K. Brown[1,2], Wilbur A. Lam[2,3,4,5], David R. Myers[3,4,5], and Oliver Brand[1,2]
[1]School of Electrical and Computer Engineering, Georgia Institute of Technology, Atlanta, Georgia, USA
[2]Institute for Electronics and Nanotechnology, Georgia Institute of Technology, Atlanta, Georgia, USA
[3]Wallace H. Coulter Department of Biomedical Engineering, Emory University & Georgia Institute of Technology, Atlanta, Georgia, USA
[4]Department of Pediatrics, Emory University, Atlanta, Georgia, USA
[5]Aflac Cancer and Blood Disorders Center, Children's Healthcare of Atlanta, Atlanta, Georgia, USA

ABSTRACT

This work presents the design, fabrication, and testing of a pillar-based microforce sensor for in-plane force sensing. The novelty of the sensor lies in its design that combines a high aspect ratio SU-8 pillar with 6µm diameter, fabricated on top of a doped silicon piezoresistor with lateral dimensions of 2x2µm or 3x3µm, which acts as the embedded active sensing element. The substrate-embedded sensing element measures the out-of-plane stress created by in-plane (transverse) forces applied to the pillar tip. A force resolution <1 µN is achieved with a lateral device footprint that is at least ten times smaller than previous MEMS force sensors. Moreover, the sensor design based on silicon piezoresistors allows for (integrated) electrical readout and scalable fabrication of sensor arrays for mechanical cell characterization.

KEYWORDS

Piezoresistor, microforce sensor, stress sensing, pillar-based sensor, in-plane force sensing, cell mechanical characterization.

INTRODUCTION

Studies of cell and tissue mechanics have shown that mechanical properties of biological cells and tissue can provide valuable information on biological processes, such as stages of cell differentiation during stem cell growth, or indicate normal or unhealthy functioning of body cells [1-3]. Mechanical characteristics of cells, such as their stiffness or contractile force, can be used as independent biomarkers in clinical diagnosis. For instance, blood platelets apply varying forces on fibrinogen protein dots during clotting processes, and the force that cell populations apply can help diagnose bleeding disorders in patients [3].

As a result, there is interest in technology and equipment that help with mechanical characterization of biological cells, tissues, and processes. Micro/nano-Newton force sensors are an important component of these tools to quantify mechanical force and stress. Considering above applications, MEMS devices are of particular interest because the device dimensions are comparable to the physical dimensions of biological cells themselves (few µm) and high force resolution is achievable. For potential diagnostic applications based on cell mechanical behavior, it is furthermore important to test large cell populations in parallel. Hence, the ability to scale, array and mass fabricate MEMS-based force/stress sensors is of importance.

However, MEMS-based force sensors that report sub-µN force resolution either have a large form factor (~100s µm to mm) or employ fabrication processes that make dense arrays and integration with CMOS circuitry difficult. As an example, Y. Sun et al. reported nano-Newton force resolution using a capacitive comb sensing mechanism using a large sensor design with millimeter dimensions [5]. Although capacitive sensors have advantages over piezoresistors in terms of noise performance and accuracy, their fabrication is generally more challenging in order to minimize and control electrode spacing. In contrast, the sub-µN force sensor designs by T. C. Duc et al. [6] and J. C. Doll et al. [7] utilize micromachined, in-plane cantilevers with embedded piezoresistors for in-plane and/or out-of-plane force sensing. The need for in-plane cantilevers again consumes valuable substrate footprint and the necessary micromachining steps for cantilever release make fabrication of dense sensor arrays challenging. An alternative, pillar-based, two-axis force sensor design demonstrated by J. C. Doll et al. [8] inspired this research. The design features two micromachined clamped-clamped cantilevers in a Swiss cross arrangement with an SU-8 pillar in the center. In-plane forces applied to the pillar bend the cantilever beams and embedded strain gauges transduce the applied force into a resistance change. However, lateral device dimensions are again in the 100s µm range, making dense arrays challenging.

SENSOR DESIGN AND FABRICATION

Sensor Design and Theory of Operation

This work presents a novel design concept for in-plane force sensing using a pillar as a mechanical cantilever structure mounted directly on top of an embedded stress-sensing element. The pillar translates a transverse, in-plane force (F_x) into an out-of-plane stress in the substrate that peaks at the base of the pillar and penetrates the underlying substrate. The novelty of the design lies in integrating doped silicon piezoresistors underneath the pillar base, which allows for a small form factor and simple fabrication process. Moreover, the piezoresistive sensing mechanism allows for device scaling and the fabrication of dense sensor arrays using a process flow that is compatible with CMOS technology.

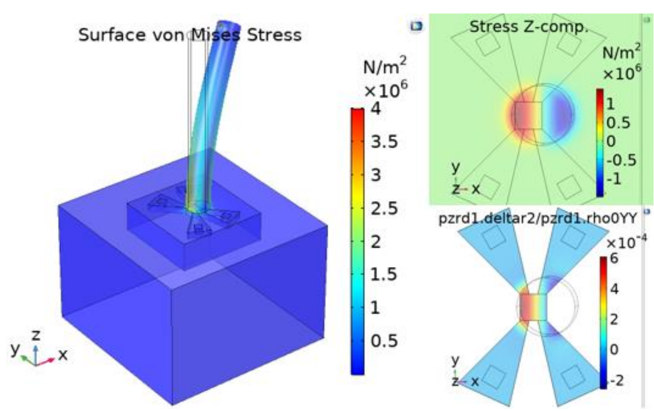

Figure 1: COMSOL FEM simulation of micro-pillar sensor with embedded 3x3µm piezoresistor: (left) von Mises stress upon 0.2µm transverse deflection of SU-8 pillar; (top right) resulting out-of-plane σ_{zz} stress 1µm deep in the plane of the piezoresistor; (bottom right) resulting simulated relative resistivity change $\Delta\rho_{yy}/\rho_0$ in the n-type silicon piezoresistor.

Finite element simulations using COMSOL as well as analytical studies were performed to investigate characteristic stress patterns and maximize the sensor output, i.e., the relative resistance change ΔR/R as a function of the applied transverse pillar force/deflection. Figure 1 shows a representative COMSOL simulation where a 0.2µm deflection is applied to the tip of an SU-8 pillar. The transverse pillar deflection creates a characteristic stress distribution in the underlying silicon substrate, with the out-of-plane stress component σ_{zz} approximately twice the magnitude of the in-plane stress components. To harvest the dominant out-of-plane stress component, we use n-doped silicon piezoresistors that have a much larger piezoresistive π_{12} coefficient compared to p-type silicon. Assuming a piezoresistor aligned with the primary flat of a (100) wafer, i.e., aligned in <110> direction, Equation (1) shows the relative resistance change ΔR/R as a function of the in-plane stress components σ_{xx}, σ_{yy} and the out-of-plane stress σ_{zz} [9]. π_{11}, π_{12} and π_{44} are the piezoresistive coefficients and the coordinate axes are aligned with the direction of the piezoresistor.

$$\frac{\Delta R}{R} = \left[\frac{\pi_{11}+\pi_{12}-\pi_{44}}{2}\right]\sigma_{xx} + \left[\frac{\pi_{11}+\pi_{12}+\pi_{44}}{2}\right]\sigma_{yy} + \pi_{12}\sigma_{zz} \qquad (1)$$

The piezoresistors are designed with four electrical contacts for four-point probing and low-noise, Kelvin measurement of the resistance. The contacts are extended out on either end of the sensing element in a "butterfly" design. This design feature and an extended contact geometry allows for access to and probing of the electrical contacts even after pillars are formed on top of the resistor.

Equation (2) highlights the maximum out-of-plane stress generated underneath the pillar as a function of the pillar height L and the pillar radius R. It is noted that the out-of-plane stress changes sign underneath the pillar (see Figure 1) and the piezoresistor must be placed off-center under one-half of the pillar base.

$$\sigma_{zz} = \frac{4}{\pi}\frac{L}{R^3}F_x \qquad (2)$$

Importantly, the z-axis stress due to a transverse force F_x is independent of the material properties of the cantilever/pillar but depends strongly on the aspect ratio of the pillar ($L/2R$) and its radius (R). Scaling the pillar dimensions while keeping the aspect ratio the same increases the maximum stress and, thus, the sensor sensitivity proportional to R^{-2}. In this work, we chose SU-8 photoresist to form the sensor pillars since the negative resist shows favorable structural properties and is easy to process. SU-8 also has the advantage of achieving high-aspect-ratio patterns with good adhesion to the silicon substrate. The pillars are formed off-center on top of the piezoresistors, with the lateral dimension of the resistor covering half the diameter of the pillar. Figure 1 highlights the relative resistivity change in the piezoresistor which has a spatial dependence because of the spatial dependence of σ_{zz}.

Fabrication Process

The fabrication process starts with a p-type (100) silicon wafer. E-beam lithography is used to define narrow (<0.4µm) trenches that outline the lateral piezoresistor edges. These trenches serve to confine the dopants introduced via solid-state diffusion to the piezoresistor body, as well as provide lateral electrical isolation of the piezoresistor from the substrate. Inductive coupled plasma (ICP) etching is used to etch the trenches (~3µm deep), outlining the piezoresistor "butterfly" geometry, using a "nano-Bosch" silicon dry etch process. The trenches are filled with oxide in a thermal oxidation step and the piezoresistor is formed in a furnace using a solid-state phosphorus (n-type) dopant source (pre-deposition step). This is followed by growth of a thermal passivation oxide layer in parallel with dopant drive-in. For formation of the four metal contacts, square openings (1x1 to 2x2µm) are etched in an isotropic wet chemical etching step. This is followed by deposition of the actual metal lines (300nm thick) via sputtering using an AlSi(1%) source. After lift-off of the excess metal, the piezoresistors are tested electrically on a four-point probe station using a semiconductor parameter analyzer (HP4155A) to measure device resistance before pillars are fabricated on top. SU-8 pillars with 6µm diameter and ~55µm height are patterned on top of the working devices using UV maskless lithography. Figure 2 shows step-by-step cross-sections of the fabrication process, along with a top view of the fabricated device prior to, and after, formation of the off-center pillar. Figure 3 shows a SEM micrograph of a fabricated butterfly device before and after SU-8 pillar fabrication.

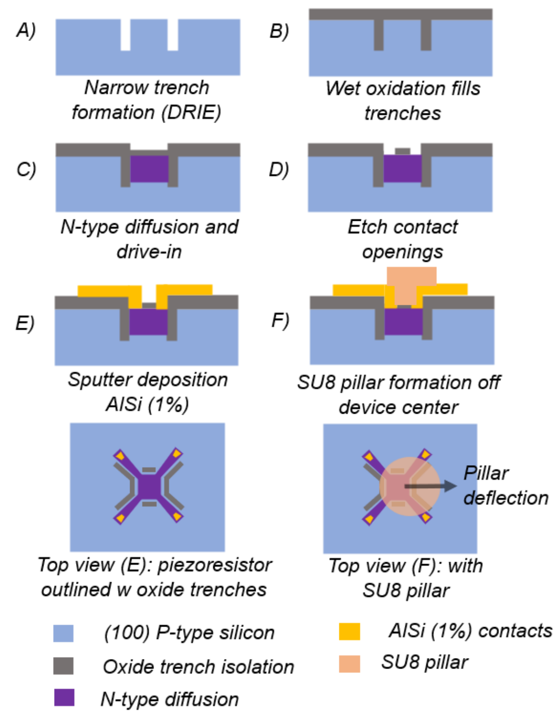

Figure 2: (A-F) Schematic cross-sections of fabrication process with p-type (100) wafer as substrate material; (bottom row) top-view schematics of completed device prior to and after SU-8 pillar fabrication.

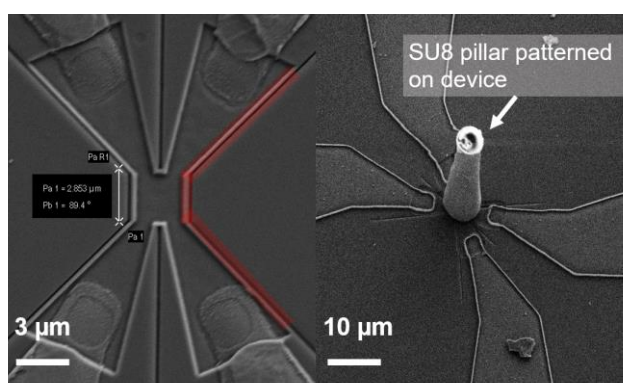

Figure 3: SEM images showing n-doped piezoresistors with extended four-point contacts in a "butterfly" design (left) without and (right) with SU-8 micropillar (5.5µm top diameter; 45µm pillar height). The red line highlights one of the oxide-filled trenches.

MECHANICAL CHARACTERIZATION

Mechanical Test Setup

For mechanical characterization of the micro-pillar sensors, a single-axis transverse displacement is applied to the tip of the SU-8 pillar while the resistance of the embedded piezoresistor is monitored in a four-point Kelvin configuration. The four-point measurement setup uses shielded triax cables and a single-channel source-meter unit (Keithley 2636A) to reduce the electrical noise in the resistance measurement. Controlled transverse deflections in steps of 0.2–0.3µm are applied to the tip of the SU-8 pillars via a stiff tungsten probe (radius 1.2µm) using the test setup schematically shown in Figure 4. The device-under-test is mounted and wire-bonded to a ceramic dual-in-line (DIL) package, which is attached to a printed circuit breakout board that connects with the source-meter unit. The tip of the tungsten probe is first aligned to the tip of the SU-8 pillar using a manual *xyz* micropositioner (MKS Newport 562-XYZ) and a high magnification lens/camera system. Once the tungsten tip is aligned with the pillar tip, a high-resolution, single-axis piezoelectric nanopositioning stage with position control (Physik Instrumente P-611.1S) applies controlled deflections to the pillar tip in *x* direction. The stage has a built-in strain gauge for position sensing and is operated in closed loop in combination with a digital controller to apply small displacements. The entire setup is screw-mounted to an air table with stiff connections improving the mechanical noise floor. During experiments, a housing shields the setup from unwanted air flow in the lab that would introduce measurement noise.

It is important to note that the displacement measured using built-in strain gauge of the single-axis nanopositioning stage is used as a measure of the tip deflection Δx applied to the SU-8 pillar. For this assumption to be correct, the effective spring constant of the mechanical connection between the nanopositioning stage and the tungsten tip has to be much larger than the spring constant of the SU-8 pillar. As shown in Figure 4, we have to consider two main spring constants connected in series, namely the springs associated with tungsten probe (K_{probe}) along with that of the probe holder (K_{holder}). The total spring constant of the setup $K_{setup} = (K_{probe}^{-1} + K_{holder}^{-1})^{-1}$ must be much larger than $K_{SU\text{-}8\ pillar}$.

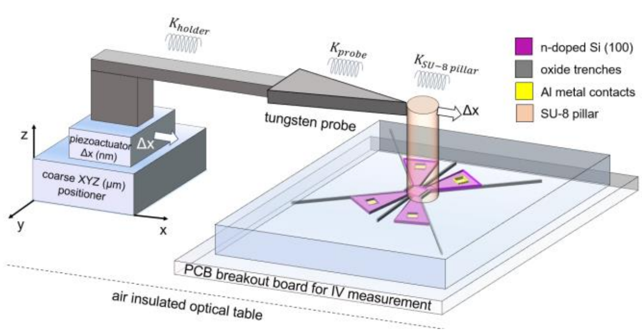

Figure 4: Schematic 3D view of the mechanical testing setup. Cross-roller bearing micromanipulators are used to position a tungsten probe in xyz with respect to the tip of the SU-8 pillar. A high magnification optical system positioned on top of the setup has a live camera to ensure proper probe and pillar alignment. After initial alignment, a closed-loop piezoactuator is used to drive the tungsten probe in sinusoidal waveforms to apply cyclic deflections to the device pillar tip. The device-under-test is wire-bonded to a dual-in-line package which is mounted to a breakout board connected to the source-meter. It is assumed that the Δx measured by the position sensor in the nanopositioning stage is equal to Δx applied to pillar.

Mechanical Characterization Results

Sensor designs of 2x2µm and 3x3µm butterfly piezoresistors with 6µm diameter, and 45-55 µm height SU-8 pillars were mechanically characterized by applying unilateral deflections in the test setup described before. The pillar geometries were kept the same for both piezoresistor dimensions to explore the effect of the piezoresistor dimension on force sensitivity. Figure 5 shows the measured relative resistance change $\Delta R/R$ of a 3x3µm piezoresistor as a function of time, while a sinusoidal deflection function with increasing and decreasing amplitude was applied to its pillar tip. The displacement measured by the position sensor embedded in the nanopositioning stage is recorded simultaneously and plotted as a second y-axis in the same graph. The device resistance responds to applied deflection within <0.2s and the measured resistance change closely follows the applied deflection.

Finally, Figure 6 presents the measured $\Delta R/R$ for each device as a function of the pillar deflection as well as a comparison with the theoretical sensitivity as simulated using COMSOL. The smaller piezoresistor yields an approx. 20% larger deflection response for the same pillar dimensions because the smaller piezoresistor is better aligned with the high-stress regions at the pillar base. The same behavior is found using COMSOL simulation. The slightly reduced experimental sensitivities compared to the COMSOL simulations are believed to be caused by alignment inaccuracies of the SU-8 pillars on top of the piezoresistors. Simulation studies confirm this dependence of the deflection sensitivity on the pillar lateral alignment to the piezoresistor.

The resulting sensitivity of the pillar-based force sensor to tip deflections, $(\Delta R/R)/\Delta x$, is 0.075%/µm and 0.090%/µm for the 3x3µm and 2x2µm piezoresistor, respectively. To obtain the device sensitivity to in-plane forces F_x applied to the pillar tip, the spring constant of the pillar was simulated using COMSOL, using the pillar dimensions of the actual sensor as obtained by SEM imaging. For the tested devices, the spring constant was simulated as $K_{SU\text{-}8pillar}$ = 8.9 N/m. For the device with 2x2µm piezoresistor, this translates into a force sensitivity, $(\Delta R/R)/F_x$ = 0.01%/µN. Furthermore, the minimum detectable deflection of 0.05µm translates into a force resolution of approximately 0.5µN. As was highlighted before, this force resolution is improved by a factor of 4 if the pillar diameter is reduced by a factor of two while keeping the aspect ratio constant.

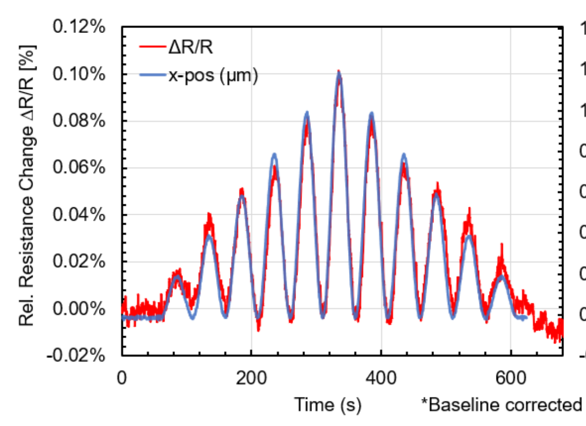

Figure 5: Measured resistance change of a 3x3µm piezoresistor with SU-8 micropillar (6µm diameter, 55µm height) undergoing sinusoidal deflections of increasing/decreasing amplitude applied by a stiff tungsten probe tip mounted to a closed-loop nanopositioner. Displayed are the simultaneously recorded relative resistance change of the piezoresistor (red) and the relative position of the nanopositioner (blue), corresponding to the tip deflection.

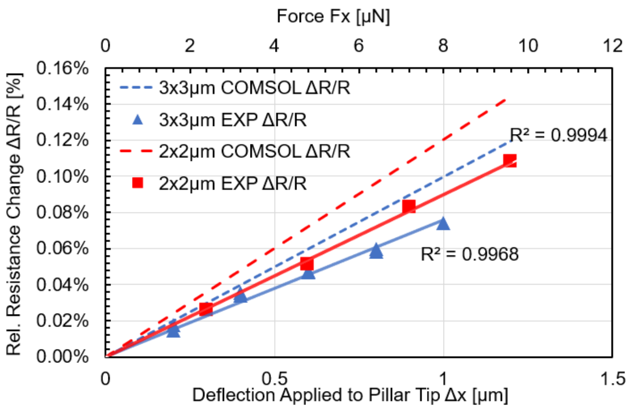

Figure 6: Average (N=3) measured relative resistance change ΔR/R for 2x2μm (red squares) and 3x3μm (blue triangles) butterfly design resistors as a function of the transverse pillar deflection Δx. The solid lines represent linear fits to the experimental data (with R^2 values), while the dashed lines are the results of the COMSOL simulation. The secondary x-axis represents the force applied to the micropillar assuming a pillar spring constant of 8.9N/m, as simulated using COMSOL.

CONCLUSION

Recent research in cell and tissue mechanics has shown that biological tissue and processes have characteristic mechanical properties (e.g., stiffness and single cell contractile forces) that can be used as independent biophysical biomarkers in clinical diagnosis. Thus, there has been a demand for micro/nano-Newton force sensing technology that help in mechanical characterization of tissue and cells as well as biological processes such as cell growth and differentiation. MEMS sensors and silicon-based CMOS fabrication technology are favorable choices to address the pressing need for biomedical lab-on-chip diagnostic and therapeutic devices because these technologies scale down to dimensions that can interface directly with individual cells. Moreover, thanks to well-developed CMOS technology, silicon-based sensing systems can be manufactured at a low-cost in large arrays for potentially testing populations of cells at a time, all alongside CMOS circuitry for single-chip signal processing.

The pillar-based, piezoresistive force sensor presented in this work has the necessary sub-μN force resolution paired with a small lateral form factor that lends itself for arraying. Moreover, the simple device fabrication that does not require micromachining release steps enables straight-forward integration with CMOS technology. Furthermore, analytical and numerical modeling highlight favorable scaling of the force sensor with the force sensitivity expected to increase proportional to R^{-2} while decreasing the pillar radius R and maintaining the pillar aspect ratio. The simple, CMOS compatible, fabrication process allows for arraying of the sensor across a single substrate to potentially form a low-cost, lab-on-chip device for testing large populations of cells.

Future work will focus on scaling down pillar and piezoresistor geometries to move towards nano-Newton force resolution as well as applying the developed sensor technology in biological applications.

ACKNOWLEDGEMENTS

This work has been funded in part by the National Science Foundation under award ECCS-1711259. The work was performed in part at the Georgia Tech Institute for Electronics and Nanotechnology, a member of the National Nanotechnology Coordinated Infrastructure (NNCI), which is supported by the National Science Foundation (ECCS-2025462). The authors would like to thank the staff of Georgia Tech's Institute for Electronics and Nanotechnology for help in device fabrication.

REFERENCES

[1] R. D. González-Cruz, V. C. Fonseca, and E. M. Darling, "Cellular mechanical properties reflect the differentiation potential of adipose-derived mesenchymal stem cells", *Proc. Natl. Acad. Sci.*, 109, E1523-E1529 (2012).

[2] Q. S. Li, G. Y. H. Lee, C. N. Ong, and C. T. Lim, "AFM indentation study of breast cancer cells", *Biochem. Biophys. Res. Commun.*, 374, 609-613 (2008).

[3] D. R. Myers, Y. Qiu, M. E. Fay, M. Tennenbaum, D. Chester, J. Cuadrado, Y. Sakurai, J. Baek, R. Tran, J. C. Ciciliano, B. Ahn, R. G. Mannino, S. T. Bunting, C. Bennett, M. Briones, A. Fernandez-Nieves, M. L. Smith, A. C. Brown, T. Sulchek and W. A. Lam, "Single-platelet nanomechanics measured by high-throughput cytometry," *Nature Materials*, 16, 230-235 (2017).

[4] H. J. Pandya, H. T. Kim, R. Roy, and J. P. Desai, "MEMS based low cost piezoresistive microcantilever force sensor and sensor module," *Material Science in Semiconductor Processing*, 19, 163-173 (2014).

[5] Y. Sun, and B. J. Nelson, "MEMS capacitive force sensors for cellular and flight biomechanics," *Biomedical Materials*, 2, S16-S22 (2007).

[6] T. C. Duc, J. F. Creemer and P. M. Sarro, "Piezoresistive Cantilever for Nano-Newton Sensing in Two Dimensions", 19th IEEE International Conference on Micro-Electro Mechanical Systems, (2006), pp. 586-589.

[7] J. C. Doll, B. C. Petzold, P. Ghale, M. B. Goodman, and B. L. Pruitt, "High frequency force sensing with piezoresistive cantilevers", Int. Solid-State Sensors, Actuators and Microsystems Conf. (Transducers 2009), (2009), pp. 1928-1931.

[8] J. C. Doll, N. Harjee, N. Klejwa, R. Kwon, S. M. Coulthard, B. C. Petzold, M. B. Goodman, and B. L. Pruitt, "SU-8 force sensing pillar arrays for biological measurements," *Lab on a chip*, 9, 1449-1454 (2009).

[9] J. Schwizer, M. Mayer and O. Brand, *Force Sensors for Microelectronic Packaging Applications*, Springer, 2004.

[10] P. Gieschke and O. Paul, "CMOS-integrated sensor chip for in-plane and out-of-plane shear stress", *Procedia Eng.*, 5, 1364-1367 (2010).

[11] A. A. Barlian, W. T. Park, J. R. Mallon, A. J. Rastegar and B. L. Pruitt, "Review: Semiconductor Piezoresistance for Microsystems", *Proceedings of the IEEE*, 97, 513-552 (2009).

CONTACT

*Oliver Brand, tel: +1-404-894-9425, oliver.brand@ece.gatech.edu